Received: 31 December 2020 | Revised: 9 June 2021 | Accepted: 14 June 2021

DOI: 10.1111/ppl.13482

SPECIAL ISSUE ARTICLE

Physiologia Plantarum

Global proteomic response of unicellular cyanobacterium *Synechocystis* sp. PCC 6803 to fluctuating light upon CO_2 step-down

Henna Mustila | Dorota Muth-Pawlak | Eva-Mari Aro | Yagut Allahverdiyeva

Molecular Plant Biology Unit, Department of Life Technologies, University of Turku, Turku, Finland

Correspondence
Yagut Allahverdiyeva, Molecular Plant Biology Unit, Department of Life Technologies, University of Turku, Turku, FI-20014, Finland.
Email: allahve@utu.fi

Funding information
Jane ja Aatos Erkon Säätiö; NordForsk, Grant/Award Number: 82845; Novo Nordisk Fonden, Grant/Award Number: NNF19OC0057634

Edited by: C. Funk

Abstract

Photosynthetic cyanobacteria are exposed to rapid changes in light intensity in their natural habitats, as well as in photobioreactors. To understand the effects of such fluctuations on *Synechocystis* sp. PCC 6803, the global proteome of cells grown under a fluctuating light condition (low background light interrupted with high light pulses) was compared to the proteome of cells grown under constant light with concomitant acclimation of cells to low CO_2 level. The untargeted global proteome of *Synechocystis* sp. PCC 6803 was analyzed by data-dependent acquisition (DDA), which relies on the high mass accuracy and sensitivity of orbitrap-based tandem mass spectrometry. In addition, a targeted selected reaction monitoring (SRM) approach was applied to monitor the proteomic changes in a strain lacking flavodiiron proteins Flv1 and Flv3. This strain is characterized by impaired growth and photosynthetic activity under fluctuating light. An obvious reprogramming of cell metabolism was observed in this study and was compared to a previous transcriptional analysis performed under the same fluctuating light regime. Cyanobacterial responses to fluctuating light correlated at mRNA and protein levels to some extent, but discrepancies indicate that several proteins are post-transcriptionally regulated (affecting observed protein abundances). The data suggest that *Synechocystis* sp. PCC 6803 maintain higher nitrogen assimilation, serving as an electron valve, for long-term acclimation to fluctuating light upon CO_2 step-down. Although Flv1 and Flv3 are known to be crucial for the cells at the onset of illumination, the flavodiiron proteins, as well as components of carbon assimilation pathways, were less abundant under fluctuating light.

1 | INTRODUCTION

Photosynthetic cyanobacteria are an important chassis for the direct conversion of light and CO_2 to value-added chemicals and fuels. In recent years, there has been growing interest in utilizing cyanobacteria and algae for the blue bioeconomy. In order to develop robust strains for efficient bioproduction, it is necessary to understand the basic physiological responses of cyanobacteria to their cultivation environment. Light intensity, quality and availability are vital factors affecting the growth and bioproduction of photosynthetic organisms. Indeed, changes in light intensity are generally able to occur (and thus impact cells) far more rapidly than abiotic stress factors, such as changing nutrient availability or temperature. Light changes can result from the mixing of water bodies and reflections of the sun, causing a

Dorota Muth-Pawlak contributed equally to this study.

lens effect on waves. As light focuses momentarily on a narrow spot below a wave in the surface water, a high-frequency light fluctuation may result (Schubert et al., 2001). Shallow coastal habitats are also known to be particularly prone to sudden sunflecks (Macintyre et al., 2000).

Rapid fluctuations in light intensity are also characteristic of conditions inside industrial-scale photobioreactors (Andersson et al., 2019; Bonnanfant et al., 2019), where high-density phototropic cultures are exposed to high light at the reactor surface and to complete darkness, due to the shading effect of cells, in the innermost area of the photobioreactor. Efficient mixing, which is necessary to ensure adequate nutrient availability, gas exchange, and light availability for the cells, exposes the cultures to light gradient and dark cycles. Therefore, an understanding of the metabolic responses of photosynthetic cells to an irregular light supply is essential for building robust cell factories for cyanobacterial bioproduction.

An array of photoprotective mechanisms enables photosynthetic organisms to survive in dynamic environments with changing light intensities. Over longer time scales, cyanobacteria can reconfigure the photosynthetic apparatus by modulating the expression level of the photosystems and by altering the phycobiliprotein pigment composition. In faster time scales, cyanobacteria can functionally reorganize their phycobilisome (PBS) antennae to regulate the light arriving at the reaction centres (reviewed by Calzadilla & Kirilovsky, 2020). Moreover, strong radiation induces an energy dissipation as heat via non-photochemical quenching (NPQ) of Chl *a* fluorescence via a soluble orange carotenoid protein (OCP) (Wilson et al., 2006).

Alternative electron transfer routes such as additional electron sinks provide another mode of protection for the photosynthetic apparatus. Cyanobacterial flavodiiron proteins (FDPs) are able to mediate electron transfer from PSI to O_2, and thus alleviate the excitation pressure of the photosynthetic electron transport chain. Upon transition from dark to light or during an increase in light intensity, a specific set of FDPs, a hetero-oligomer formed by Flv1 and Flv3, provides a rapid and powerful electron sink from the downstream of PSI (Allahverdiyeva et al., 2013; Bulychev et al., 2018; Helman et al., 2003). In *Synechocystis* sp. PCC 6803 (hereafter *Synechocystis*), Flv2/Flv4 heterodimer also catalyzes the light induced reduction of O_2, although with lower activity but by continuously sustaining O_2 uptake at least for 5–10 min (Santana-Sanchez et al., 2019). Flv1/Flv3 hetero-oligomers have shown to be crucial for photoreduction of O_2 as a fast response to excessive reduction of PSI and enable cell survival under fluctuating light intensities when the growth light is repeatedly interrupted by high light pulses (Allahverdiyeva et al., 2013; Santana-Sanchez et al., 2019).

Another versatile electron transfer component is a multi-subunit NAD(P)H dehydrogenase-like complex (NDH-1), mainly localized in thylakoid membranes (Laughlin et al., 2020; Peltier et al., 2016). NDH-1 plays a role as an alternative electron transport pathway contributing to redox homeostasis and protection of photosynthesis. In cyanobacteria, four NDH-1 types with specific subunits have been identified: NDH-1_1 and NDH-1_2 functioning in respiration and NDH-1_3 and NDH-1_4 functioning in carbon concentration mechanism (CCM) (Peltier et al., 2016). All four NDH-1 types catalyze cyclic electron transfer (CET) around PSI by distributing electrons between reduced ferredoxin (Fdx) and plastoquinone (PQ) (Schuller et al., 2020). Recently, functional redundancy between NDH-$1_{1,2}$ and Flv1/Flv3 was suggested in *Synechocystis*; both complexes accept electrons from reduced Fdx and contribute to photoprotection of photosynthesis (Nikkanen et al., 2020).

Recently various "omics" studies, such as transcriptomics or proteomics, have been applied to understand the global cellular responses in cyanobacteria (Babele et al., 2019; Jahn et al., 2018; Zavřel et al., 2019). While changes in gene expression are important to understand cell regulation at the transcript level, protein abundance can directly reflect the cell metabolism and regulation at a particular point in time. Alterations in transcript levels are much faster than for proteins, and mRNA and protein levels for specific genes and pathways are not always well correlated (Maier et al., 2009; Palenik, 2015; Vogel & Marcotte, 2012). The existence of a large number of post-translational modifications and the differences between turnover rates of proteins strongly suggests that monitoring global regulation mechanisms and complex cell metabolism based on an integrated omics approach provides a reliable and in-depth understanding of the cell metabolism.

Previously, we showed that intermittent light induces a multitude of differential changes in the transcriptome of *Synechocystis* (Mustila et al., 2016). In this study, we investigate the global proteome response of cells to intermittent light upon concomitant acclimation to air-level CO_2 by applying a label free untargeted mass spectrometry quantification by data-dependent acquisition (DDA) to *Synechocystis* wild-type (WT) and, as a follow-up experiment, using targeted mass spectrometry approach as selected reaction monitoring (SRM) to the Δ*flv1*/Δ*flv3* deletion mutant. We applied the same experimental setup as in the previous transcriptome study (Mustila et al., 2016), allowing us to determine how well the changes in transcript level are reflected in protein expression. Application of both transcriptomics or proteomics techniques simultaneously is advantageous to avoid misinterpretations. In this work, we show that *Synechocystis* modulate the carbon and nitrogen balance in response to rapidly changing light intensities. As a long-term acclimation strategy to the intermittent light *Synechocystis*, WT maintains nitrogen assimilation pathways as an electron sink, while the Δ*flv1*/Δ*flv3* mutant is unable to apply WT strategy to adjust to fluctuating light.

2 | MATERIAL AND METHODS

2.1 | Strains, culture conditions, and sampling

The wild-type (WT) and Δ*flv1*/Δ*flv3* strain (Allahverdiyeva et al., 2011) of *Synechocystis* sp. PCC 6803 were cultivated in 30 ml BG-11 (Rippka et al., 1979), supplemented with 20 mM Hepes-NaOH, pH 7.5 in 100 ml Erlenmeyer flasks in AlgaeTron AG 130-ECO growth chamber (PSI, Czech) at 30°C. Cultures were shaken at 150 rpm and illuminated with LED white light. Pre-experimental cultures were

grown under constant illumination of 50 μmol photons m^{-2} s^{-1} Photosynthetically Active Radiation (PAR) and supplemented with 3% CO_2 (HC). After 2 days, pre-cultures were harvested, ODs of the experimental cultures were adjusted, and the cells were shifted to ambient air level CO_2 (LC). The cultures were grown either under fluctuating light intensities (20 μmol photons m^{-2} s^{-1} background light was interrupted every 5 min by 500 μmol photons m^{-2} s^{-1} for 30 s, FL20/500) or moderate constant light (50 μmol photons m^{-2} s^{-1}, CL) for 48 h (Figure 1A, Table 1). Since *Synechocystis* WT cultures grow more slowly under the applied fluctuating light (Mustila et al., 2016), the initial OD was adjusted higher (OD_{750} = 0.4) than for the constant light-grown cultures (OD_{750} = 0.2). Under constant light, WT cultures reached OD_{750} = 0.57 ± 0.02 in 48 h. It is known that the growth of the Δ*flv1*/Δ*flv3* mutant is completely inhibited by a small inoculum size (OD_{750} = 0.1) under FL20/500 fluctuating light (Figure S1A, Allahverdiyeva et al., 2013, Mustila et al., 2016). In order to create comparable conditions and allow the Δ*flv1*/Δ*flv3* cells to grow, the initial OD_{750} was adjusted to 0.4 for both WT and Δ*flv1*/Δ*flv3*. The WT grew to an OD_{750} of 0.77 ± 0.002, whereas the Δ*flv1*/Δ*flv3* cultures reached only an OD_{750} of 0.50 ± 0.03 in 48 h (Figure S1B).

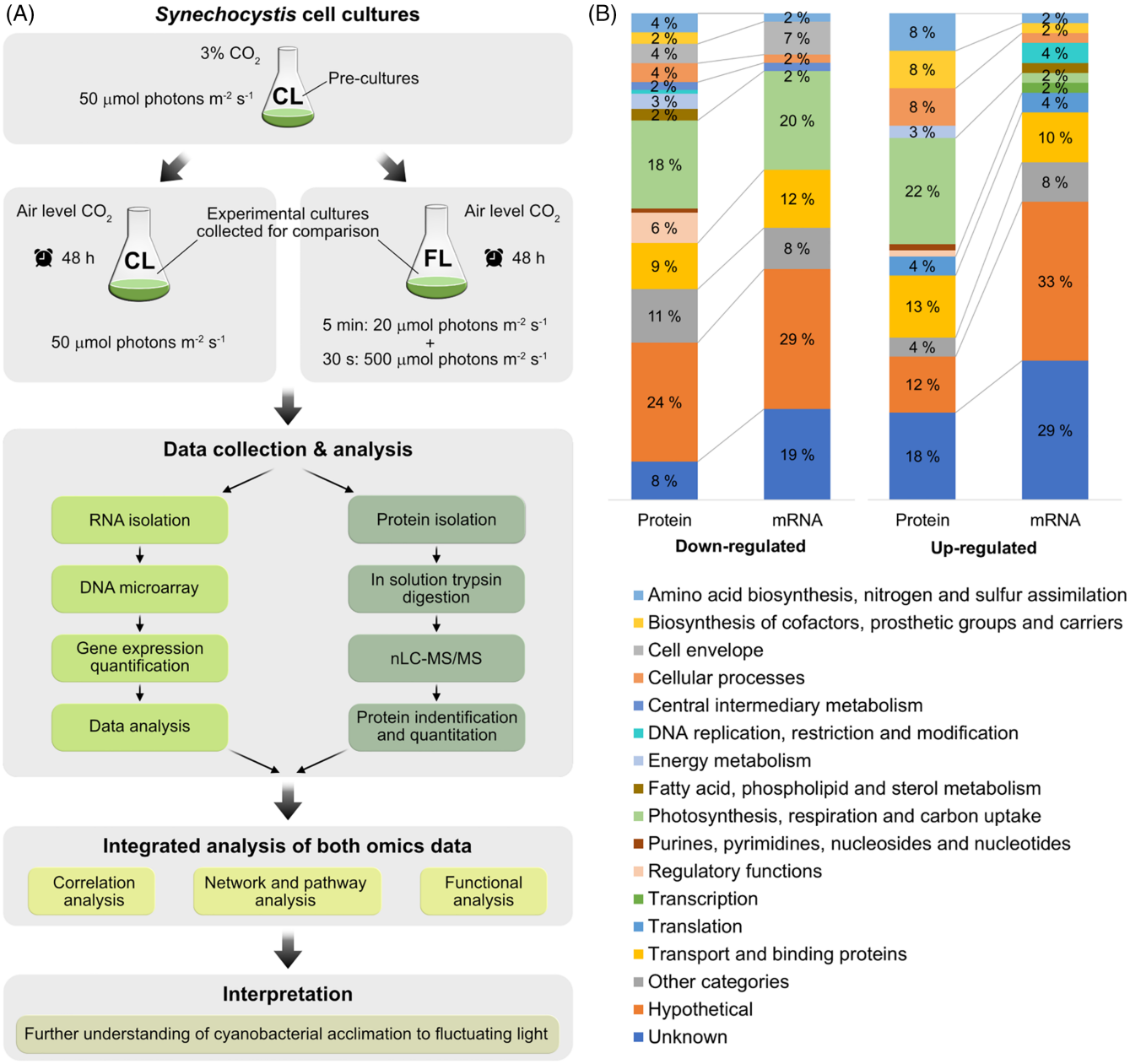

FIGURE 1 The protein and gene expression analysis in *Synechocystis* WT grown under fluctuating light (FL20/500) compared with the WT grown under constant light (CL) during CO_2 step-down. (A) A schematic diagram describing the DDA and microarray experimental design. (B) Differential protein and transcript expression divided in functional categories. The proteome was analyzed with DDA in this study, whereas microarray data were published previously (Mustila et al., 2016). DDA analysis was done with cut-off threshold $\log_2$FC ≥ 0.58 or ≤−0.58 (which corresponds to FC = ±1.5) and transcript analysis with cut-off threshold −1 ≤ $\log_2$FC ≥ 1, both data sets with *P*-value ≤ 0.05

TABLE 1 Summary of the growth conditions used in this study

	Pre-culture conditions		Experimental culture conditions				
Sample	Light	CO_2	Light	CO_2	Collection time	Protein analysis	Transcript analysis
CL	Constant growth light: 50 μmol photons m^{-2} s^{-1}	3%	Constant growth light: 50 μmol photons m^{-2} s^{-1}	Air	48 h	This study	1)
FL	Constant growth light: 50 μmol photons m^{-2} s^{-1}	3%	Fluctuating light: 5 min: 20 μmol photons m^{-2} s^{-1} 30 s: 500 μmol photons m^{-2} s^{-1}	Air	48 h	This study	1)

Note: Synechocystis WT and Δ*flv1*/Δ*flv3* strain were grown under constant light (CL) or under fluctuating light (FL) in BG-11 medium supplemented with 20 mM Hepes-NaOH (pH 7.5). Pre-experimental cultures were grown with 3% CO_2, while experimental cultures were kept under air level of CO_2. The microarray data used in comparison here have been previously published in 1) Mustila et al. (2016)

Experimental cultures were cultivated under atmospheric CO_2 level, and sodium carbonate was omitted from the BG-11 medium. After 48 h, the cells were harvested by centrifugation at 4°C. The cell pellet was washed twice with 50 mM TES-KOH (pH 8.0) and then stored at −80°C for further treatment. The absence of contamination was checked by spreading liquid culture on LB and R2A agar plates.

2.2 | Sample preparation

The samples were prepared according to the protocol described in Vuorijoki et al. (2016). The proteins extracted from *Synechocystis* cells were reduced by 5 mM dithiothreitol (DTT) and alkylated with 10 mM iodoacetamide (IAA) before precipitation with 1:5 v/v of 50% acetone/50% ethanol o/n at −20°C. The proteins were digested on-pellet with two portions of trypsin in 1:100 enzyme to protein added in 4 h interval. After overnight incubation with trypsin, peptides mixture was further desalted and injected on LC–MS/MS in biological triplicate and technical duplicate.

2.3 | DDA quantification

DDA was performed on an EASY-nLC 1000 nanoflow liquid chromatography coupled to a Q Exactive mass spectrometer (Thermo Fisher Scientific). Extracted peptides equivalent to 250 ng were first loaded on a trapping column (0.3 × 5 mm PepMap C18, LC Packings) and subsequently separated inline on a 15 cm C18 column (75 mm × 15 cm, ReproSil 5 μm 200 Å C_{18}, Dr. Maisch GmbH, Ammerbuch-Entringen, Germany). The mobile phase consisted of water/acetonitrile (98:2 [v/v]) with 0.1% formic acid (solvent A) or acetonitrile/water (95:5 [v/v]) with 0.1% formic acid (solvent B). A stepped 110 min gradient (70 min 5–26% B, 30 min 26–49% B, 5 min 49–100% B and 5 min 100% B) was used to elute peptides. The Q Exactive instrument was operated with Thermo Xcalibur software (Thermo Fisher Scientific) in positive mode with a spray voltage of 2.3 kV. The survey scan (MS) with the detection range of 300–2000 m/z was followed by MS/MS scan of up to 10 most intense ions with charge higher than +2 with the resolution of 120,000 and 15,000 (m/z 200), respectively. The fragmentation was performed in HCD cell with normalized collision energy of 27%. The automatic gain control (AGC) settings were set to a maximum fill time of 100 ms and 250 ms and to obtain a maximum number of 3e6 and 1e5 ions for MS and MS/MS scans, respectively. The raw files were searched against *Synechocystis* protein database retrieved from Cyanobase (Kaneko et al., 1996) supplemented with human and yeast proteome retrieved from Uniprot database, using in-house Mascot (v.2.4)—search engine (Perkins et al., 1999) and further analyzed using Proteome Discoverer™ (v.1.4) Software (Thermo Scientific™). The Mascot search parameters were set to trypsin as an enzyme with two miscleavages allowed, methionine oxidation as variable modification and carbamidomethylation as the fixed one. Precursor mass tolerance was restricted to monoisotopic mass ±4 ppm and fragment ion to ±0.02 Da. For the validation of the spectrum identifications, Percolator (Käll et al., 2007) algorithm was used with a relaxed false discovery rate (FDR) of 0.05. The mass spectrometry proteomics data have been deposited to the ProteomeXchange Consortium (Deutsch et al., 2017) via the PRIDE partner repository with data-set identifier PXD023066 and 10.6019/PXD023066 (Vizcaíno et al., 2016).

Label-free DDA quantification was performed using Progenesis QI for proteomics, LC–MS 4.0 (Nonlinear Dynamics). Only proteins identified with ≥2 unique peptides were considered, and ANOVA *P*-value ≤0.05 was used as statistical significance threshold.

2.4 | SRM quantification

The SRM protein quantification was performed according to the protocol described previously (Vuorijoki et al., 2016). Samples after pellet digestion and desalting (see Sample preparation) were injected into the LC–MS in biological triplicate. The data were analyzed in Skyline (3.1.0.7382) (MacLean et al., 2010) software, and statistics were performed in the MSstats (3.1.4) package (Choi, Chang, Clough, et al., 2014; Choi, Chang, & Vitek, 2014). Peptide abundances were measured using the nanoLC system (EasyNanoLC 1000, Thermo Fisher Scientific) coupled to a triple quadrupole mass spectrometer (TSQ Vantage, Thermo Scientific) equipped with a nanoelectrospray source. Samples were loaded onto a pre-column (75 μm × 2 cm, 3 mm 120A°C18, Reprosil-Pur, Dr. MaischGmbH), then eluted and separated on an analytical column (75 μm × 15 cm, 3 mm, 120A°C18,

Reprosil-Pur, Dr. MaischGmbH) using a 60 min non-linear gradient at a flow rate of 300 nl min^{-1} (5–20% B in 35 min; 20–35% B in 50 min; B-acetonitrile: water, 98:5). The transitions were measured with a 2.0 s cycle time, 0.7-unit resolution for both quadrupoles (Q1 and Q3), and the isolation width of 0.002 m/z. The mass spectrometer operated in SRM positive mode with a spray voltage of 1600 V, 270°C capillary temperature, collision gas pressure of 1.2 mTorr argon in Q2 and tuned at the S-lens value.

2.5 | Absorption spectroscopy

In situ absorption spectra (370–750 nm) of cell suspensions were recorded by the OLIS CLARiTY 17 UV/VIS/NIR spectrophotometer with the integrating cavity (On Line Instrument Systems, Inc.) that allows correction for cellular scattering. The raw absorbance data were converted into absorbance values by using Fry's method (Fry et al., 1992).

3 | RESULTS

In order to understand major changes in cell metabolism under intermittent light, we performed a global protein expression analysis in *Synechocystis* WT grown both under fluctuating light intensities (FL20/500, 20 µmol photons m^{-2} s^{-1} (PAR) background light was interrupted every 5 min by 500 µmol photons m^{-2} s^{-1} for 30 s) and moderate constant light (CL, 50 µmol photons m^{-2} s^{-1}) for 48 h. It is important to highlight that pre-cultures were grown under 3% CO_2; therefore, the effect of fluctuating light is studied during the acclimation to air-level CO_2. Unfractionated cell lysates were subjected to in solution digestion, and the peptides were quantified with nanoflow liquid chromatography–tandem mass spectrometry (nLC-MS/MS). The total proteome of *Synechocystis* WT was analyzed using the label-free DDA technique (Figure 1A). We have previously used the same experimental setup for microarray studies (Mustila et al., 2016), which allowed a complementary profiling of gene expression and proteomic responses. In both cases, the cells were sampled only after they had acclimated to the experimental conditions (48 h), enabling better comparison with transcripts and proteins.

The MS-based quantitative protein analysis covered 1499 proteins, each with at least two peptides. In total, 128 proteins were found to be downregulated and 78 upregulated upon exposure to fluctuating light (cut-off $log_2FC \geq 0.58$ or ≤ -0.58 and $P < 0.05$). From this group, there were five proteins with lower abundance and seven with higher abundance, which had not been included in our previous DNA microarray analysis, which excluded plasmid encoded genes (Mustila et al., 2016). The differentially expressed proteins and genes responding to fluctuating light are visualized as volcano plots in Figure 2A,B. Of the differentially expressed proteins, 28 of the corresponding genes were significantly downregulated (23.1%) and seven genes upregulated (10.1%). Thus, on average, 16.6% of the altered mRNA level showed the same response in protein level.

In general, proteins classified into functional categories of photosynthesis as well as transport and binding demonstrated notable expression responses both as transcripts and proteins. These proteins are specified and compared to their transcript abundances described in Mustila et al., 2016 (see Table 2). Proteins involved in nitrogen assimilation, transport, and cellular processes also demonstrated notable expression responses to the fluctuating light condition (Table 2). The relative portion of proteins and genes in separate functional categories showed different abundances under fluctuating light compared to constant light (Figure 1B, Tables S1 and S2). The functional categories in Figure 1B are based on the categories determined in Cyanobase; however, some of the proteins are reorganized to other categories based on functionality determined in more recent literature. Many of the proteins and genes showing different abundances under fluctuating light compared to constant light are unknown or hypothetical in their function (Figure 1B).

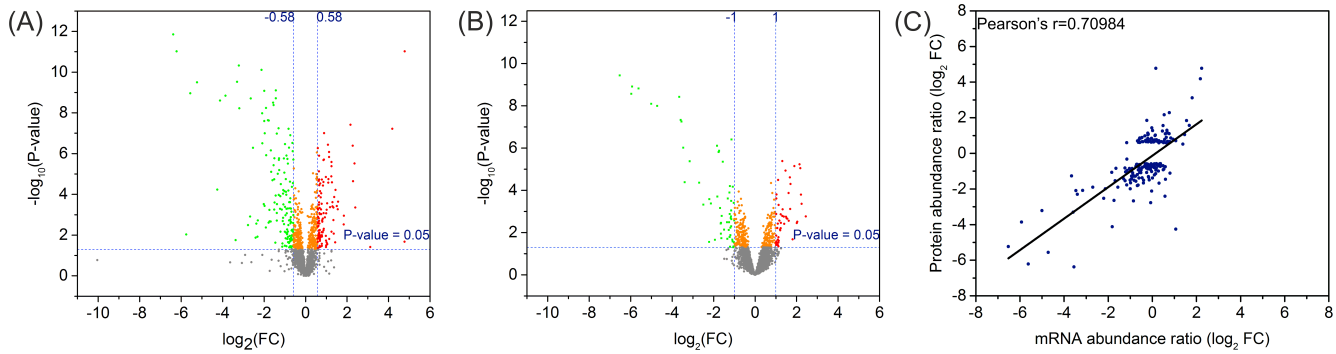

FIGURE 2 Differentially expressed transcripts and proteins under fluctuating light. Volcano plots of fold change in protein (A) and transcript (B) abundance in WT under fluctuating light (FL20/500) compared to constant growth light (CL) during CO_2 step-down. The proteome was analyzed with DDA in this study, whereas microarray data were published previously (Mustila et al., 2016). DDA analysis was done with cut-off threshold $log_2FC \geq 0.58$ or ≤ -0.58 and transcript analysis with cut-off threshold $log_2FC \geq 1$ or ≤ -1, both data sets with *P*-value ≤0.05.
(C) Scatterplot of the correlations between protein and mRNA expression. Pearson's correlation between the differentially expressed proteins and their corresponding mRNAs was $r = 0.71$

TABLE 2 Proteins quantified with the DDA compared to transcripts quantified with DNA microarray

Accession	Gene	Protein Log_2FC This study	RNA Log_2FC Mustila et al. (2016)
Photosynthesis and respiration			
Photosystem I			
sll0634	*btpA*	**0.86**	**−0.51**
Photosystem II			
sll0258	*psbV*	**0.67**	0.24
slr0144	NA	**0.74**	−0.30
slr0146	NA	**0.67**	0.69
slr0147	NA	**0.70**	0.30
slr0149	NA	**0.69**	0.13
slr0151	NA	**0.75**	0.12
slr1544	lilA	**4.77**	**2.24**
Phycobilisome			
slr2067	*apcA*	**0.78**	0.56
slr1986	*apcB*	**0.66**	0.52
sll0928	*apcD*	**0.90**	0.63
slr1459	*apcF*	**0.64**	0.32
Soluble electron carriers			
sll0199	*petE*	**0.59**	0.63
ssl0020	*fdx1*	**1.14**	0.65
FDPs			
sll1521	*flv1*	ND	0.14
sll0219	*flv2*	**−3.22**	**−5.00**
sll0550	*flv3*	**−1.99**	**−1.00**
sll0217	*flv4*	**−3.86**	**−5.93**
NADH dehydrogenase			
sll0519	*ndhA*	**−1.27**	−0.94
sll0223	*ndhB*	**−0.99**	**−0.95**
sll0522	*ndhE*	**−1.29**	−0.76
sll0521	*ndhG*	**−1.65**	−0.99
slr0261	*ndhH*	**−1.43**	**−0.94**
sll0520	*ndhI*	**−1.54**	**−1.23**
slr1281	*ndhJ*	**−1.54**	**−1.68**
slr1280	*ndhK*	**−1.43**	−1.29
slr1623	*ndhM*	**−1.67**	−0.40
sll1262	*ndhN*	**−1.51**	**−0.82**
ssl1690	*ndhO*	**−1.30**	−0.18
sll0272	ndhV	**−1.49**	−0.14
sll1733	*ndhD3*	**−2.08**	**−3.15**
sll1732	*ndhF3*	**−2.30**	**−3.40**
sll1734	*cupA*	**−1.91**	**−2.70**
sll1735	*cupS*	**−1.99**	**−2.13**
sll0027	*ndhD4*	**1.56**	0.49
slr1302	*cupB*	**2.16**	**0.54**

Accession	Gene	Protein Log_2FC This study	RNA Log_2FC Mustila et al. (2016)
Nitrogen assimilation			
sll0108	*amt1*	**1.30**	0.66
slr0447	*urtA*	**2.28**	**0.77**
slr1201	*urtC*	**0.86**	**0.84**
sll0764	*urtD*	**0.86**	−0.57
sll0374	*urtE*	**1.14**	−0.20
sll0450	*norB*	**−4.12**	**−1.82**
sll1454	*narB*	**1.57**	**1.68**
slr0898	*nirA*	**1.08**	−0.19
ssl1911	*gifA, IF7*	**−2.78**	−0.07
sll1515	*gifB, IF17*	**−4.26**	1.07
slr0288	*glnN, GS*	**4.78**	0.16
slr0899	*cynS*	**1.10**	0.77
slr1898	*argB*	**0.65**	−0.28
slr2002	*cphA*	**0.59**	**−1.16**
ssl2667	*nifU*	**−1.78**	**−0.64**
Transport and binding proteins			
sll0507	*corA*	**1.04**	−0.19
sll0672	*pacL*	**−1.38**	−0.61
sll0689	*nhaS3*	**−0.99**	**−0.99**
sll1270	*bgtB*	**0.65**	−0.46
slr0454	*acrB*	**0.69**	−0.09
slr1046	*tatB*	**−0.67**	0.08
slr1247	*pstS2*	**−0.75**	−0.08
slr1295	*idiA*	**1.00**	0.12
slr1452	*sbpA*	**−2.67**	−0.85
slr2043	*znuA*	**−0.85**	**−1.65**
Translation			
slr1808	*hemA*	**0.88**	−0.47
sll1394	*msrA*	**0.64**	0.06
slr0955	NA	**0.52**	**1.39**
Biosynthesis of cofactors			
sll1091	*chlP*	**0.64**	−0.04
sll1282	*ribH*	**1.25**	0.46
slr0118	*thiC*	**0.65**	−0.43
slr0426	*folE*	**−0.73**	0.37
slr0502	*cobW*	**−0.59**	−0.05
slr0772	*chlB*	**0.67**	0.30
slr0900	*moeA*	**1.18**	**0.67**
slr1562	*grxB*	**−0.79**	0.08
slr1992	*gpx2*	**0.60**	**0.69**
Cell envelope			
sll0016	*mltA*	**−1.90**	**−1.56**
slr1351	*murF*	**−1.77**	**−1.16**

TABLE 2 (Continued)

Accession	Gene	Protein Log_2FC	RNA Log_2FC	Accession	Gene	Protein Log_2FC	RNA Log_2FC
Carbon assimilation				*slr1423*	*murC*	**−0.68**	−0.17
sll1031	*ccmM*	**−0.64**	−0.59	*slr1924*	*pbp7*	**−1.81**	**−0.68**
sll1032	*ccmN*	**−0.93**	−0.63	**Cellular processes**			
slr0009	*rbcL*	**−0.95**	−0.52	*sll1294*	*taxD2*	**−0.63**	−0.55
slr0012	*rbcS*	**−1.22**	−0.88	*sll1514*	*hspA*	**3.12**	**1.81**
sll0834	*bicA*	**4.18**	**2.18**	*sll1980*	*trxA*	**−0.75**	−0.09
slr0040	*cmpA*	**−5.23**	**−6.53**	*sll1987*	*katG*	**0.76**	0.19
slr0041	*cmpB*	**−6.22**	**−5.62**	*slr0904*	*comM*	**−0.97**	**−1.14**
slr0043	*cmpC*	**−3.30**	**−3.58**	**CRISPR2**			
slr0044	*cmpD*	**−6.38**	**−3.55**	*sll7066*	*cas7*	**0.76**	PE
slr0042	*porB*	**−5.56**	**−4.72**	*sll7069*	NA	**1.25**	PE
slr1512	*sbtA*	**−2.09**	**−3.46**	*sll7070*	NA	**0.71**	PE
slr1513	*sbtB*	**−1.27**	**−3.66**	*slr7073*	NA	**0.64**	PE
Other functions							
sll0221	*prxQ2*	**−1.02**	−0.03	*sll6055*	NA	**−2.02**	PE
sll1224	*hoxY*	**−0.77**	−0.28	*slr0006*	NA	**−2.53**	**−2.20**
sll1268	*urf*	**0.83**	−0.20	*slr0427*	NA	**−0.65**	0.23
sll1483	NA	**1.84**	**1.56**	*slr1261*	NA	**1.02**	0.14
sll1507	NA	**0.70**	−0.67	*slr2004*	NA	**−1.08**	−0.25
sll1951	*HlyA*	**0.62**	−0.05	*slr2032*	*ycf23*	**−2.12**	−0.03
sll5075	NA	**−1.23**	PE	*ssr1528*	NA	**−2.64**	**−1.74**

Note: Synechocystis WT grown under fluctuating light (FL20/500) is compared to WT grown under constant light. Pre-experimental cultures were grown under 3% CO_2, while experimental cultures were kept under air level of CO_2. Transcripts and proteins $P \leq 0.05$ are shown with bold font, colored background shows blue for downregulated and red for upregulated. Protein data analysis of DDA was treated with cut-off threshold $P \leq 0.05$ and $log_2FC \geq 0.58$ or ≤ -0.58.
Abbreviations: NA, not available; ND, not detected; PE, plasmid encoded.

3.1 | Fluctuating light induces expression of proteins associated with photosynthesis

As shown in Table 2, several proteins associated with photosynthesis and the assembly of photosystems were in higher abundance under fluctuating light. The transcripts of many of the proteins identified here showed similar trends, but their induction was not recognized as statistically significant (Mustila et al., 2016). The following proteins were identified to have differential expression: (1) The PSI biogenesis protein BtpA, which post-transcriptionally regulates the translation of *psaAB* mRNA and stabilizes the reaction centre core proteins PsaA/PsaB of PSI (Bartsevich & Pakrasi, 1997; Zak & Pakrasi, 2000); (2) Cytochrome c550 (PsbV), a PSII extrinsic protein required for stabilization of the Mn cluster of the oxygen evolving complex (Roncel et al., 2012; Shen et al., 1998); (3) Soluble electron carriers, ferredoxin 1 (Fdx1) and plastocyanin (PetE), which were abundant at protein level under fluctuating light, while the transcript amounts were equal in constant and fluctuating light (Table 2). Since Fdx1 is a crucial distributor of electrons to both Calvin-Benson-Bassham (CBB) cycle enzymes via ferredoxin-$NADP^+$ oxidoreductase (FNR) and to alternative electron transport routes, a higher amount of Fdx1 might alleviate the excitation pressure to PSI. Among the electron acceptors from reduced Fdx1, only NDH-1_4, nitrite reductase (NirA), and nitrate reductase (NarB) showed significantly higher abundances at both the transcript and protein levels under fluctuating light. Other electron acceptors downstream of PSI, such as flavodiiron proteins (FDPs) and bidirectional hydrogenase (Hox) showed lower abundance. The Flv3 protein and heterodimer of Flv2/Flv4 proteins did show lower expression both at protein and transcript levels. The downregulation of FDPs under fluctuating light has been previously verified with Western immunoblot analysis (Mustila et al., 2016). Moreover, the accumulation of the HoxY subunit of bidirectional hydrogenase was slightly diminished. (4) Intriguingly, several PBS core proteins (ApcA, ApcB, ApcD and ApcF) were found in higher abundance under fluctuating light, which was not visible at the transcript level. Typically, PBSs size and thus abundances of proteins associated with light harvesting diminished with increasing light intensity and growth rate (Zavřel et al., 2019). Downregulation of genes encoding for phycobiliproteins and PSI has been reported also at transcript level upon exposure to constant high light (Muramatsu & Hihara, 2012).

(5) PSII assembly factors Slr0144, Slr0147, and Slr0149 together with two other PSII-related proteins Slr0146 and Slr0151, all encoded from a Pap-operon (PSII assembly proteins), were induced (Heinz et al., 2016; Wegener et al., 2008). One of the most enhanced in amounts, both at protein and transcript level, was LilA that is a member of the extended light-harvesting-like (Lil) protein family. LilA has been found to be associated specifically with PSII (Kufryk et al., 2008). LilA and other members of the Hlips (high light-induced proteins) family are associated with photoprotection of photosystems against excess light energy (Muramatsu & Hihara, 2012). In addition, IdiA (Iron deficiency induced protein A) was found in higher amounts under fluctuating light. IdiA has also been found associated with PSII in *Synechocystis* (Tölle et al., 2002), and the IdiA homolog in *Synechococcus* sp. PCC 7942 has been suggested to play a role in protecting the acceptor side of PSII under oxidative stress (Exss-Sonne et al., 2000) and under iron or manganese deficiency (Michel et al., 1996). High levels of PSII assembly factors encoded by the Pap-operon suggest a faster turnover of PSII proteins. The enhancement of LilA and IdiA proteins indicates possible protection mechanisms for both PSII and PSI complexes under fluctuating light. In addition, geranylgeranyl reductase ChlP functioning in Chl *a* and tocopherol biosynthesis pathway was found at higher levels under fluctuating light.

3.2 | Expression of components in carbon and nitrogen assimilation responds to fluctuating light

Two major metabolic pathways, carbon and nitrogen assimilation, responded inversely to fluctuating light with concomitant CO_2 step-down. Fluctuating light conditions resulted in high amounts of most of the components in nitrogen uptake and assimilation, including nitrate and nitrite reductases (NarB and NirA, respectively), glutamine synthetase (GS) Type III encoded by *glnN*, ABC transporters for urea (Urt) and an ammonium translocator (Amt) (Table 2). Also, the amount of cyanophycin synthetase that is responsible for the accumulation of the nitrogen reserve cyanophycin was observed at higher abundance. The amino acid L-arginine biosynthesis was also abundant based on upregulation of acetylglutamate kinase ArgB. Consistent with other findings, GS inactivating factors IF7 and IF17 were found in lower abundance. Intriguingly, the strong induction of GS and repression of IF7 and IF17 was found only at protein level, while subunits of the urea and ammonium transporters were more abundant as both transcripts and proteins.

Coordinated reduction of both transcripts and proteins was recorded for several components of carbon assimilation (Table 2). Fluctuating light applied upon CO_2 step-down led to reduced amounts of low inorganic carbon (Ci)-inducible NDH-1_3, while NDH-1_4 functioning in constitutive CO_2 uptake was more abundant at both the transcript and protein levels. Low Ci inducible HCO_3^- transporters BCT1 and SbtA in the plasma membrane and a probable porin (PorB) in the outer membrane and corresponding transcripts were also less abundant. CcmM and CcmN, essential for carboxysome formation, and Rubisco subunits were found to be at lower levels. Only BicA, a low-affinity bicarbonate transporter, was strongly enhanced at transcript and protein level under fluctuating light in comparison to constant light. It is of note that, unlike transcripts of the subunits of BCT1 and SbtA, the mRNA amount of *bicA* is not induced upon Ci deprivation (Klähn et al., 2015). It is highly possible that, as a consequence of pre-experimental growth of the cells under 3% CO_2, the experimental cultures shifted to air level CO_2 under fluctuating light were not able to induce as strong CCM as the constant light cultures due to the dominance of abrupt changes signaled by the initiation of fluctuating light conditions. As a comparison, during the shift of *Synechocystis* cultures from 3% to air level of CO_2 under constant moderate light illumination, the majority of proteins, including those of CCM, were shown to reach a new steady-state expression level during 24–72 h (Battchikova et al., 2010). Abrupted low Ci induced CCM signaling under fluctuating light, in comparison to constant light conditions, would explain the repression of the low Ci inducible components of CCM (NDH-1_3, BCT1, and SbtA), and possibly also the higher abundance of constitutively expressed CCM components (BicA and NDH1_4) (Table 2).

3.3 | Fluctuating light triggers limited photoprotective mechanisms

Intriguingly, among the multitude of proteins scavenging reactive oxygen species (ROS) in cyanobacteria (Latifi et al., 2009; Schmitt et al., 2014), a catalase-peroxidase KatG and glutathione peroxidase Gpx2 were found more abundant under fluctuating light (Table 2). The KatG catalase-peroxidase is the only catalase present in *Synechocystis* and able to detoxify H_2O_2 (Tichy & Vermaas, 1999). The NADPH-dependent glutathione peroxidases, Gpx1 and Gpx2, reduce unsaturated fatty acid hydroperoxides under normal and oxidative stress conditions to protect membrane integrity (Gaber et al., 2001, 2004). Besides the catalase and two glutathione peroxidases, *Synechocystis* possess five thioredoxin-dependent peroxiredoxins, and one of them, PrxQ2 (Sll0221), showed reduced content in fluctuating light as compared to constant light. Unlike the four other peroxiredoxins, PrxQ2 is postulated to be a lumenal or periplasmic protein (Pérez-Pérez et al., 2009). Heat shock proteins (HSPs) are also typically induced by various stress reactions; however, we found only HspA strongly enhanced by fluctuating light.

It is noteworthy that the OCP-mediating NPQ (reviewed by Kirilovsky & Kerfeld, 2016) or chaperonins encoded from the *groESL* operon were found not to be more abundant, in either the WT or Δ*flv1*/Δ*flv3* strain under fluctuating light (Tables 2 and 3). These results are in agreement with findings by Muramatsu and Hihara (2012), demonstrating that the expression of *hspA* is induced by sensing the reduced state of the plastoquinone (PQ) pool, while expression of certain stress responsive genes, including *groESL* and *ocp*, is induced in response to sensing the reduced state of electron transfer components located downstream of the PQ pool. Even though OCP is thought to be important under high light, a short 30 s high light pulse was not enough to enhance its expression to a greater

TABLE 3 Proteins quantified with the SRM compared to transcripts quantified with DNA microarray

Accession	Gene	Protein	RNA
		Log_2FC	Log_2FC
		This study	Mustila et al. (2016)
Photosystem I			
slr1835	*psaB*	**−0.55**	−0.40
slr1655	*psaL1*	**−0.70**	−0.96
Soluble electron carriers			
ssl0020	*fdx1*	**−2.42**	**−1.54**
sll0199	*petE*	**−0.53**	−0.55
sll0662	*fdx7*	**1.35**	0.05
FDPs			
sll0219	*flv2*	**−0.78**	1.36
sll0217	*flv4*	**−0.83**	**1.60**
NADH dehydrogenase			
sll1733	*ndhD3*	**−1.43**	0.02
sll1732	*ndhF3*	**−1.22**	−0.02
sll1734	*cupA*	**−1.45**	−0.40
sll1594	*ndhR*	**−1.32**	0.18
CCM			
slr0436	*ccmO*	**0.74**	**0.67**
sll0030	*cmpR*	**−0.93**	−0.15
slr1512	*sbtA*	**−2.99**	−1.08
Respiratory terminal oxidases			
slr1136	*coxB*	**−0.80**	−0.21
slr1379	*cydA*	**−1.19**	−0.60
Nitrogen assimilation			
sll1451	*nrtB*	**−1.65**	**−1.80**
sll1452	*nrtC*	**−0.99**	**−1.82**
sll1453	*nrtD*	**−1.06**	**−2.25**
sll1454	*narB*	**−0.62**	**−2.02**
slr0447	*urtA*	**−0.90**	**−1.83**
Other functions			
slr1738	*perR*	**1.04**	**1.01**
sll0221	*prxQ2*	**−2.46**	**−0.58**
slr1198	*1-cys prx*	**0.71**	−0.57
sll1223	*hoxU*	**2.16**	0.48
sll0891	*citH*	**0.62**	0.42
slr0884	*gap1*	**−0.74**	**−0.70**

Note: Δ*flv1*/Δ*flv3* strain grown under fluctuating light (FL20/500) is compared to WT grown under fluctuating light during CO_2 step-down. Transcripts and proteins $P \leq 0.05$ are shown with bold font, colored background shows blue for downregulated and red for upregulated. Protein data analysis of SRM was treated with cut-off threshold $P \leq 0.05$ and $-0.53 \leq \log_2FC \geq 0.58$.

extent than what was observed after a shift from 3% CO_2 to air level CO_2 under constant light (Battchikova et al., 2010). In agreement with our results, the maximum capacity for OCP-mediated NPQ was measured for *Synechocystis* grown in a photobioreactor with highly variable light intensity, with a lack of significant NPQ induction during the day (Andersson et al., 2019).

CRISPR2-system associated proteins Slr7073, Sll7066 (Cas7), Sll7069 and Sll7070 were among the proteins that showed higher relative abundance in response to fluctuating light. These proteins represent one of the three CRISPR-Cas systems in *Synechocystis*, all of the corresponding genes located in a native pSYSA plasmid (Scholz et al., 2013). Clustered regularly interspaced short palindromic repeats (CRISPR) and CRISPR-associated (Cas) protein systems are suggested to provide adaptive immunity against invading phages and resistance to horizontal gene transfer in many bacteria and archaea; however, the exact function of the CRISPR-Cas system is still elusive (reviewed by Sontheimer & Marraffini, 2010; Hille et al., 2018). Transcription factor RpaB has been predicted to activate CRISPR2 genes among many other redox responsive genes (Riediger et al., 2019). Whether the upregulation of the CRISPR2-system noted here is a direct response to the fluctuating light remains still uncertain.

Intriguingly, nitric oxide reductase (NorB) was present at a considerably lower amount and HoxY at a slightly lower amount in the WT under fluctuating light (Table 2). The membrane bound NorB uses electrons provided by quinols to reduce nitric oxide (NO) to nitrous oxide (N_2O) and putatively protects bacteria from the toxic NO (Büsch et al., 2002). It has been shown previously that the regulatory protein CyAbrB2 negatively regulates both the *norB* and *hox* operon (Leplat et al., 2013), while it acts as a positive regulator for several nitrogen-regulated genes such as *urtA*, *amt1*, *narB*, and the *nrt* operon (Ishii & Hihara, 2008). However, CyAbrB2 was also found to positively regulate CCM-related genes (*cmpABCB*, *sbtAB*, and *ndhF3/ndhD3/cupA* operons) and complement CmpR and NdhR transcription factors (Orf et al., 2016). In *Synechocystis*, NorB activity might be related to detoxification of NO deriving from the endogenous nitrite reductase activity or the nitrite reducing process of other phytoplankton. However, the reason for the strong repression of NorB in response to intermittent light is not clear, but might be connected to the overall response of the CyAbrB2 regulon and CO_2 step-down.

3.4 | SRM provides quantitative insight into the response of Δ*flv1*/Δ*flv3* strain to fluctuating light

The function of Flv1/Flv3 hetero-oligomer was previously shown crucial for the viability of *Synechocystis* under fluctuating light (Allahverdiyeva et al., 2013). Therefore, we also monitored the changes in the proteome profile of Δ*flv1*/Δ*flv3* under intermittent light in comparison to WT. Here we applied a recently established targeted MS-based SRM method to detect changes in protein amounts (Vuorijoki et al., 2016). With SRM, we were able to quantify certain photosynthetic proteins that were missing from the DDA quantification: subunits for thylakoid membrane-localized cytochrome *c* oxidase (Cox) and *bd*-quinol oxidase (Cyd), the reaction centre protein for PSII (PsbAII) and transcriptional regulators (CmpR and PerR). In general, SRM offers better analysis for low abundant and

membrane bound proteins. As the target peptides are selected, the instrument is focused on monitoring only the corresponding ion channels, thus omitting interfering signals and therefore enabling more sensitive and accurate measurement than the DDA technology.

It is noteworthy that the Δ*flv1*/Δ*flv3* mutant is unable to grow, from a low inoculum size (OD_{750} = 0.1), under FL20/500 fluctuating light under conditions of 3% CO_2 (Figure S1A), air level CO_2 (Mustila et al., 2016), or during the shift from HC to LC (Allahverdiyeva et al., 2013). However, the Δ*flv1*/Δ*flv3* cells can survive under FL20/500 with a larger (OD_{750} = 0.4) inoculum size, although the growth is slower compared to the WT (Figure S1B). In order to collect enough biomass for current fluctuating light experiments, both WT and Δ*flv1*/Δ*flv3* cells were inoculated at OD_{750} = 0.4 and cultivated for 48 h.

Altogether 86 proteins were targeted and quantified with the SRM approach. From these, 20 proteins were significantly downregulated and seven upregulated in Δ*flv1*/Δ*flv3* compared to WT grown under intermittent light (Tables 3 and S3). Different from the acclimation strategy applied by WT under intermittent light, the Δ*flv1*/Δ*flv3* mutant demonstrated diminished levels of Fdx1 and proteins of nitrogen assimilation pathway (NrtB-D) compared to WT, which is in accordance with microarray data described in the previous study (Mustila et al., 2016). Components of NDH-1_3 (NdhD3, NdhF3, CupA), SbtA, and transcriptional regulator NdhR were also less abundant. However, these components were not as significantly lowered as transcripts in Δ*flv1*/Δ*flv3* compared to the WT under fluctuating light (Mustila et al., 2016). Considering that all of these CCM components were already significantly repressed in the WT in response to fluctuating light during CO_2 step-down (Table 2), and further downregulated in Δ*flv1*/Δ*flv3* compared to WT, it is conceivable that low transcript and protein abundances prevailed both in Δ*flv1*/Δ*flv3* and WT cells under fluctuating light. Very low transcript amounts might explain why microarray analysis did not reveal changes for these genes, whereas at the protein level the diminished abundance can be recorded by sensitive SRM approach. In addition, NdhD2 and CmpA-C proteins were under the detection limit and could not be quantified with SRM from either WT or Δ*flv1*/Δ*flv3* cells grown under fluctuating light conditions. The *cmpA-D* operon was significantly downregulated also at the transcript level in WT under fluctuating light (Mustila et al., 2016). Interestingly, NdhD2 showed an opposite response at transcript and protein level since downregulation was detected only at the protein level.

The PsaB, Flv2, and Flv4 proteins showed lower content in Δ*flv1*/Δ*flv3* compared to WT under fluctuating light, which is all in accordance with earlier immunoblot detection (Table 3 and Mustila et al., 2016). In addition, PsaL1, PSI protein, and plastocyanin were less abundant. Surprisingly, the amounts of CoxB and CydA were also diminished in Δ*flv1*/Δ*flv3* cells in comparison to WT. These respiratory terminal oxidases can function as an electron valve under light, although with low sink capacity (Ermakova et al., 2016). From possible electron sinks only HoxU, the diaphorase subunit of the bidirectional hydrogenase was enhanced in Δ*flv1*/Δ*flv3* cells (Table 3). However, we did not detect the other subunits of the hydrogenase (Artz et al., 2020).

From the significantly abundant proteins in response to fluctuating light (Table 3), PerR, a peroxide-sensing repressor, was similarly upregulated also as a transcript. PerR was shown to be induced by H_2O_2 and function as a transcriptional regulator of peroxiredoxin PrxII (Li et al. 2004). Moreover, a cytosolic peroxiredoxin, 1-Cys Prx, was enhanced while the putatively lumenal PrxQ2 was diminished. Ferredoxin 7 (Fdx7), playing a role in the protection against hydrogen peroxide (Cassier-Chauvat & Chauvat, 2014) and photooxidative stress (Mustila et al., 2014), was found in larger amounts.

3.5 | Changes in the pigment composition induced by fluctuating light

Enhanced allophycocyanin (ApcA,B,D,F) content detected in WT and changes in the abundance of certain PSI subunits (PsaB, PsaL) in Δ*flv1*/Δ*flv3* under FL20/500 intermittent light point out possible differences in the cellular content of photosynthetic pigments (Tables 2 and 3). To analyze the pigment composition, in situ room temperature absorption spectra were recorded from the cultures grown under constant light or fluctuating light conditions for 48 h. While the WT cells showed slightly elevated phycobilin content (peak at 626 nm), the Δ*flv1*/Δ*flv3* cells showed a clear decrease in phycobilin and Chl *a* (peaks at 440 nm and 680 nm) content under fluctuating light compared to constant light (Figure 3). Carotenoid (peak at 480–490 nm) ratio to Chl *a* remained unchanged for WT, while Δ*flv1*/Δ*flv3* cells showed increased carotenoids under fluctuating light compared to constant light (Figure S2B,C). Importantly, the characteristics of the pigmentation were similar when precultures were cultivated under 3%

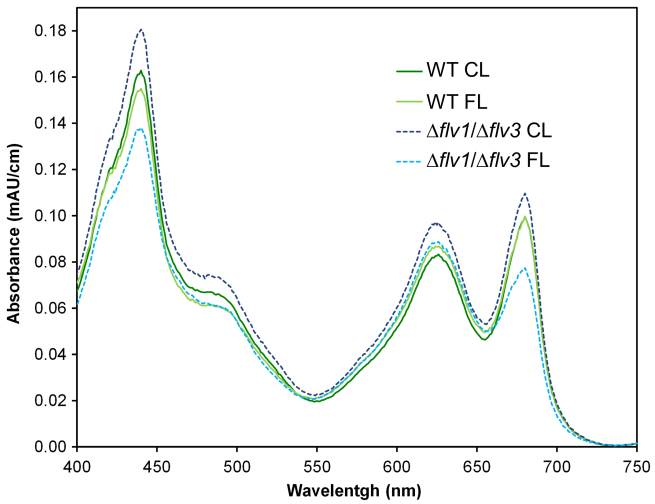

FIGURE 3 Whole cell absorption spectra of the wild-type (WT) and Δ*flv1*/Δ*flv3* strain. Cells were pre-cultivated under 3% CO_2, adjusted to OD_{750} = 0.2 or 0.4 for cultivating under constant light or fluctuating light (FL20/500) for 48 h under ambient CO_2, respectively. Before recording the absorption spectra, OD_{750} was adjusted to 0.2

(Figure 3) or air level of CO_2 (Figure S2A-C), implying that the modifications in the pigment composition were a response to fluctuating light regardless of the CO_2 level used for precultivations.

4 | DISCUSSION

The majority of omics studies addressing acclimation of cyanobacteria to low or high light intensities have been performed under constant light regimes both for the analysis of transcriptomes (Hihara et al., 2001; Muramatsu & Hihara, 2012; Tan et al., 2018) and proteomes (Choi et al., 2000; Jahn et al., 2018; Zavřel et al., 2019). However, both in nature and in densely populated photobioreactors, cyanobacterial cells will rarely experience a constant growth light condition. Our aim in this study was to mimic fluctuations in irradiance, although in a controlled manner, and to reveal strategies that cells may apply to cope during intermittent light. In addition, we compare differences induced by fluctuating light in global protein expression to previously described transcriptome results (Mustila et al., 2016). Despite the transcriptomics study being performed earlier, the strain, culture conditions, growth chamber, and sampling times were all identical. This allowed for a reliable comparison of the two omics data sets.

4.1 | Correlation of proteome and transcriptome in response to fluctuating light

The amount of common regulation observed between transcripts and proteins varies among cyanobacterial studies, with our results exhibiting a relatively high correlation ($r = 0.71$) (Figure 2C). As a comparison, Frischkorn et al. (2019) studied phosphorous stress and found that only approximately 10% of identified global proteins showed co-expression with genes identified in transcriptome analysis for the cyanobacterium *Trichodesmium erythraeum*. In a similar (non-global) study, 37% of transcripts and proteins detected were significantly downregulated in a similar manner in response to inorganic phosphorus stress in *Anabaena* sp. strain 90 (Teikari et al., 2015). The Pearson's correlation coefficients between transcriptomics and proteomics results were 0.75, with a data-set size of 47 identified protein spots on 2D gels. In a study analyzing the cyanobacterial response to high light stress, the proteomics analysis covered approximately half of the predicted proteins in the *Synechococcus* sp. PCC 7002 proteome (Xiong et al., 2015). In their integrated analysis, the correlation of transcripts and proteins was observed to be rather low (Pearson's correlation $r = 0.24$). However, considering all quantified proteins and their corresponding mRNAs, while calculating the correlations only for differentially expressed proteins, the correlation was higher ($r = 0.41$) (Xiong et al., 2015). As a comparison to studies in Eukaryotic cells, the mRNA-protein correlation for *Saccharomyces cerevisiae* was found to vary between studies ($r = 0.36–0.76$) as reviewed in Maier et al. (2009).

Relatively weak correlations between the amounts of mRNA and protein abundances are commonly observed (Maier et al., 2009; Nie et al., 2007; Toyoshima et al., 2020; Wegener et al., 2010). Changes in transcriptome might be very rapid and induced by the stress response, while changes in protein abundances might take hours or days. In the current study, the relatively high correlation observed between proteins and transcripts might be explained by the strong stress applied and by the acclimation time. In general, a higher degree of correlation of the global transcriptome in relation to the proteome has been observed after introducing strong stress, rather than upon mild stress (Halbeisen & Gerber, 2009; Waldbauer et al., 2012). Some of the inconsistency might be explained by methodological aspects and some may be inherent with the sample. Expression of mRNA is a prerequisite for protein translation, but there are a variety of post-transcriptional regulations, for example, small regulatory RNAs and folding of secondary structures in RNA molecules, which affect the half-life of transcripts and ribosome accessibility to mRNA (Muro-Pastor & Hess, 2020).

Moreover, translation efficiency depends on translation initiation and bias in codon usage (Chemla et al., 2020; Maier et al., 2009). The third level is post-translational control, which affects the activity and half-life of proteins. For example, protein phosphorylation and inherent protein stability result in different protein turnover rates. In photosynthetic protein complexes in the model plant *Arabidopsis thaliana*, certain subunits have shown very rapid protein degradation and subsequent replacement with newly synthesized protein (Li et al., 2018). These include the D1 protein of PSII and PetD in cytochrome b_6f complex, both supposedly linked to the photoprotection of these complexes in photosynthetic electron transport. The current methodology does not allow conclusions to be drawn regarding the dynamics of conformational changes of the proteome, nor to measure activity or composition of the complexes. Both DDA and SRM approaches have their limitations. While DDA is biased toward highly abundant proteins, SRM is low throughput. Nevertheless, with both methods, it is possible to gain insight into overall changes in protein abundances in photosynthetic cells.

4.2 | Enhanced nitrogen assimilation serves as an electron valve under fluctuating light upon CO_2 step-down

Our global proteomic analysis revealed coordinated reprogramming of the major metabolic pathways in WT *Synechocystis* in response to rapidly changing light intensities with concomitant CO_2 step-down (Figure 4). Overall, the proteins participating in nitrogen transport and assimilation were more abundant under the FL20/500 light regime. Among the highly abundant nitrogen assimilation pathway components, nitrite reductase (NirA) and nitrate reductase (NarB) use reduced Fdx as an electron donor (Flores & Herrero, 2005). Nitrate reductase catalyzes a two-electron reaction to reduce nitrate to nitrite, followed by a six-electron reaction catalyzed by nitrite reductase to produce ammonium (Flores et al., 1983). Accordingly, nitrate

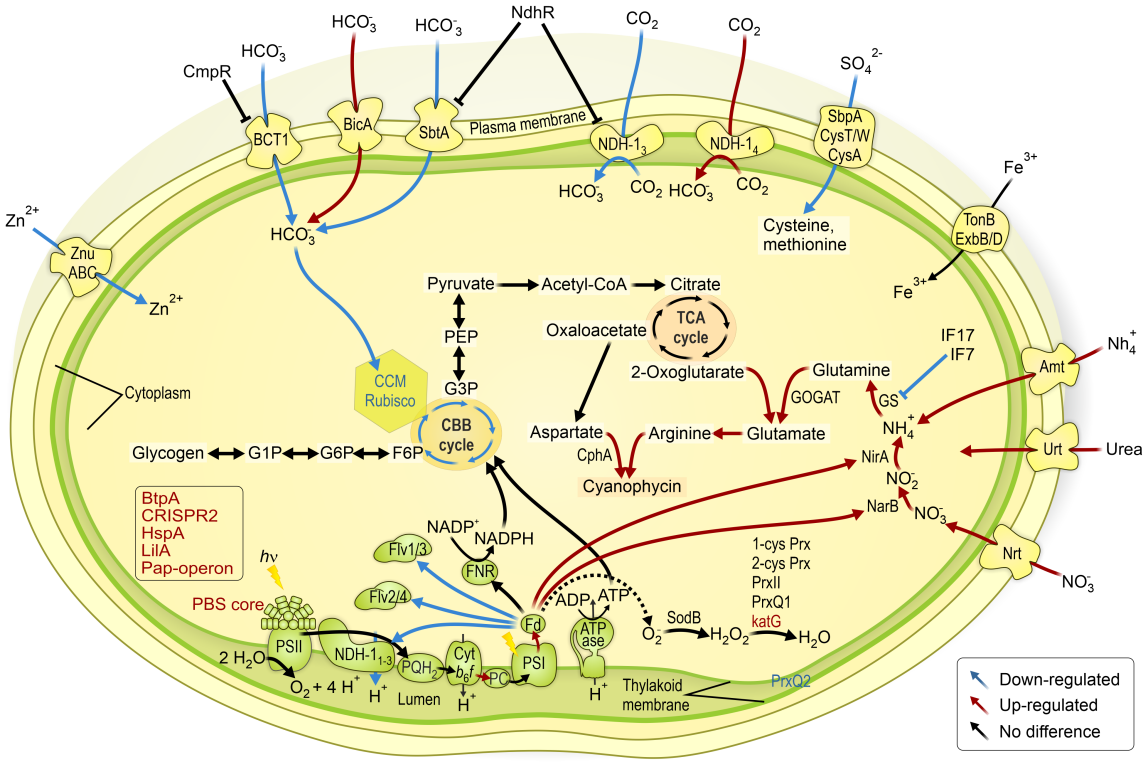

FIGURE 4 Schematic showing changes in the metabolism of *Synechocystis* cells under fluctuating light (FL20/500) upon CO_2 step-down. Cells were pre-cultivated under 3% CO_2, adjusted to $OD_{750} = 0.2$ or 0.4 for cultivating under constant light or fluctuating light (FL20/500) for 48 h, respectively. More abundant proteins and pathways are marked with red, and less abundant proteins and routes are marked with blue

reduction has been shown to function as an important electron sink (Klotz et al., 2015). The data obtained in this study suggest that increased nitrogen assimilation could serve as a strong electron valve under the fluctuating light regime.

Nitrogen compounds are also important for PBS and maintenance of the photosystems, and accordingly, under fluctuating light, the core subunits of PBS and many PSII assembly proteins were more abundant than under continuous light after a shift from 3% to air level CO_2. The elevated phycobilin content under fluctuating light was confirmed by the whole cell absorption spectra (Figures 3 and S2). The Chl *a* content was equal in both light regimes for WT (Figure 3), and no changes in the subunits of photosynthetic complexes were detected (Table 2), indicating that cells did not adjust the content of Chl *a* binding pigment complexes in response to fluctuating light. These findings are in agreement with previous observations (Allahverdiyeva et al., 2013), showing that the photochemical quantum yield of PSII Y(II) and the yield of PSI Y(I) for WT were similar both under fluctuating light and constant light. Thus, there were no major adjustments for photosynthetic electron transport in response to fluctuating light. Instead, other cell metabolism acclimation processes occur (these are summarized in Figure 4).

Among the components of the alternative electron transport route, three FDPs (Flv3 and the heterodimer forming Flv2/Flv4 proteins) did show lower expression level in the WT cells exposed to fluctuating light (Table 2). This observation is counterintuitive, as we have previously demonstrated the crucial role of Flv1 and Flv3 proteins under fluctuating light conditions (Figure S1, Allahverdiyeva et al., 2013; Mustila et al., 2016). The repression of these electron transport components could, in part, be due to the low background light used in our fluctuating light set up, which would also explain the enhancement of the antenna proteins. However, repression of FDPs has previously been seen after a shift to FL50/500 fluctuating light with a higher background intensity (50 μmol photons m^{-2} s^{-1}), although to a lesser extent (Mustila et al., 2016) compared to FL20/500 used in this study. In this study, we used 3% CO_2 for pre-cultivation of cells and the effect of fluctuating light is studied 48 h after a drop to air level CO_2 conditions. A significant increase in the abundance of FDPs (except Flv1) along with CCM proteins upon a shift to LC has been shown previously (Battchikova et al., 2010; Spät et al., 2021). Contrasting this, under the studied fluctuating light intensities with CO_2 step-down, WT *Synechocystis* cells demonstrated low abundances of CCM proteins and FDPs. Fluctuating light might interrupt signaling and prevent induction of certain low CO_2 inducible proteins upon the shift from high to low CO_2 conditions. However, this cannot fully explain the decline in amounts of FDPs or NdhD3 under FL20/500, because a similar response was also detected when cells were pre-cultured under air levels of CO_2 prior to transfer to fluctuating light (Figure 2A in Mustila et al., 2016). Recently, Nikkanen et al. (2020) demonstrated functional redundancy between Flv1/Flv3 and NDH-1 in PSI protection in *Synechocystis*. The close relationship between FDPs and CCM is also supported by the fact that cyclic electron flow and FDP-mediated water–water cycle energize the CCM through the generation of a trans-thylakoidal *pmf* in the green alga *Chlamydomonas reinhardtii* (Burlacot et al., 2021). However, the

exact mechanism behind the decrease of FDPs under fluctuating light is not clear.

Importantly, SRM analysis revealed that, unlike WT cells, the Δ*flv1*/Δ*flv3* mutant is unable to maintain high nitrogen assimilation under the FL20/500 regime, demonstrating diminished levels of nitrogen transport and assimilation proteins (Table 3) and transcripts (Mustila et al., 2016). Moreover, the reaction centre protein PsaB showed reduced levels, accompanied by substantially reduced Chl *a* and phycobilin content under fluctuating light (Table 3, Figure 3). Consequently, a lack of Flv1/Flv3 route and repressed nitrogen assimilation increase the acceptor side limitation of PSI and lead to detrimental effects on cell viability of the Δ*flv1*/Δ*flv3* strain under long-term intermittent light (Allahverdiyeva et al., 2013, Mustila et al., 2016).

The different response of the WT and Δ*flv1*/Δ*flv3* strain to nitrogen assimilation under fluctuating light and concomitant lowering of the CO_2 level implies differences in signaling to regulate these pathways. As intracellular carbon:nitrogen (C/N) homeostasis is vital to optimal cell growth, the carbon and nitrogen metabolism is tightly regulated (reviewed in Forchhammer & Selim, 2019). 2-oxoglutarate (2-OG), an intermediate from the TCA cycle, acts as a signal of nitrogen status mediated by the global nitrogen control factor NtcA. In addition, 2-OG together with $NADP^+$ serves as a signal of inorganic carbon limitation to a major transcriptional regulator NdhR (Daley et al., 2012). Therefore, 2-OG status can be seen as a central indicator of the C/N balance. Interestingly, a recent study demonstrated that H_2O_2 interferes with C/N status sensing by affecting the 2-OG levels (Robles-Rengel et al., 2019). It is conceivable that in the Δ*flv1*/Δ*flv3* strain, oxidative stress is more pronounced than in the WT due to a lack of electron sinks, with H_2O_2 then impending induction of nitrogen assimilation. Here, *Synechocystis* exposed to fluctuating light demonstrated upregulation of HspA and peroxidases (KatG and Gpx2), and the Δ*flv1*/Δ*flv3* strain showed higher abundance of PerR, 1-cys prx and Fdx7, all contributing to the alleviation of the effects of oxidative stress. These findings are in line with earlier results showing a higher level of oxidative damage to proteins upon exposure to fluctuating light, both for WT cells and, more noticeably in the Δ*flv1*/Δ*flv3* strain (Allahverdiyeva et al., 2013). Taken together, these results indicate that crosstalk between FDPs and nitrogen assimilation could be possible. Despite FDPs being known to function as NO quenchers in anaerobic microbes and *Chlamydomonas reinhardtii* (Burlacot et al., 2020), the possible involvement of cyanobacterial FDPs in N-metabolism and NO-reduction has yet to be considered. NO could act as a signaling molecule between photosynthetic apparatus and N-metabolism.

5 | CONCLUSIONS

The global proteomic analysis presented in this work has revealed a coordinated reprogramming of the major metabolic pathways in *Synechocystis* in response to rapidly and periodically changing light intensities upon CO_2 step-down. Several components in carbon assimilation and CCM were found at lower amounts and nitrogen assimilation pathways were found to be more abundant both at transcript and protein level. We postulate that *Synechocystis* uses an enhanced nitrogen assimilation pathway as a long-term acclimation strategy to intermittent light. This serves as an alternative electron valve under fluctuating light and alleviates the excitation pressure on the photosynthetic apparatus. The lower abundance of FDPs is applied as a long-term strategy since to rely only on the water-to-water-cycle as a safety valve would be energetically unfavorable (due to the wasting of photosynthetic electrons) to the cells under these challenging conditions. Although overall global proteomic analysis correlated with earlier transcriptomic findings, individual components in the pathways did not correlate in every instance, thus, suggesting wide post-transcriptional and post-translational regulation. Taken together, label-free MS detection combined with SRM can serve as a reliable approach for cyanobacterial protein quantification and allow comprehensive evaluation of the cell metabolism.

ACKNOWLEDGMENTS

The authors thank the Biocenter Finland and the Proteomics Facility of the Turku Bioscience center for the support. This research was funded by the NordForsk Nordic Center of Excellence "NordAqua" (no. 82845 to Y.A.), the Academy of Finland (no. 315119 to Y.A), Novo Nordisk Foundation project "PhotoPro" (no. NNF19OC0057634 to Y.A.), and Jane and Aatos Erkko Foundation (to EM.A.). The authors would like to thank Dr. Dmitry Shevela (ShevelaDesign AB, Umeå, Sweden) for preparation of Figure 4.

AUTHOR CONTRIBUTIONS

Yagut Allahverdiyeva and Eva-Mari Aro conceived the study. All authors were involved in designing the experiments. Henna Mustila and Dorota Muth-Pawlak conducted the experiments and analyzed the data. Dorota Muth-Pawlak performed proteomics. Henna Mustila and Yagut Allahverdiyeva wrote the manuscript with input from all authors.

DATA AVAILABILITY STATEMENT

The data that support the findings of this study are openly available in ProteomeXchange Consortium via the PRIDE partner repository with dataset identifier PXD023066 and 10.6019/PXD023066.

ORCID

Henna Mustila https://orcid.org/0000-0002-1939-7197
Dorota Muth-Pawlak https://orcid.org/0000-0001-7005-2007
Yagut Allahverdiyeva https://orcid.org/0000-0002-9262-1757

REFERENCES

Allahverdiyeva, Y., Ermakova, M., Eisenhut, M., Zhang, P., Richaud, P., Hagemann, M. et al. (2011) Interplay between flavodiiron proteins and photorespiration in *Synechocystis* sp. PCC 6803. *The Journal of Biological Chemistry*, 286, 24007–24014.

Allahverdiyeva, Y., Mustila, H., Ermakova, M., Bersanini, L., Richaud, P., Ajlani, G. et al. (2013) Flavodiiron proteins Flv1 and Flv3 enable cyanobacterial growth and photosynthesis under fluctuating light. *Proceedings of the National Academy of Sciences of the United States of America*, 110, 4111–4116.

Andersson, B., Shen, C., Cantrell, M., Dandy, D.S. & Peers, G. (2019) The fluctuating cell-specific light environment and its effects on cyanobacterial physiology. *Plant Physiology*, 181, 547–564.

Artz, J.H., Tokmina-Lukaszewska, M., Mulder, D.W., Lubner, C.E., Gutekunst, K., Appel, J. et al. (2020) The structure and reactivity of the HoxEFU complex from the cyanobacterium *Synechocystis* sp. PCC 6803. *The Journal of Biological Chemistry*, 295, 9445–9454.

Babele, P.K., Kumar, J. & Chaturvedi, V. (2019) Proteomic de-regulation in cyanobacteria in response to abiotic stresses. *Frontiers in Microbiology*, 10, 1–22.

Bartsevich, V.V. & Pakrasi, H.B. (1997) Molecular identification of a novel protein that regulates biogenesis of photosystem I, a membrane protein complex. *The Journal of Biological Chemistry*, 272, 6382–6387.

Battchikova, N., Vainonen, J.P., Vorontsova, N., Keränen, M., Carmel, D. & Aro, E.M. (2010) Dynamic changes in the proteome of *synechocystis* 6803 in response to CO_2 limitation revealed by quantitative proteomics. *Journal of Proteome Research*, 9, 5896–5912.

Bonnanfant, M., Jesus, B., Pruvost, J., Mouget, J.L. & Campbell, D.A. (2019) Photosynthetic electron transport transients in *Chlorella vulgaris* under fluctuating light. *Algal Research*, 44, 101713.

Bulychev, A.A., Cherkashin, A.A., Muronets, E.M. & Elanskaya, I.V. (2018) Photoinduction of electron transport on the acceptor side of PSI in *Synechocystis* PCC 6803 mutant deficient in flavodiiron proteins Flv1 and Flv3. *Biochimica et Biophysica Acta - Bioenergetics*, 1859, 1086–1095.

Burlacot, A., Dao, O., Auroy, P., Cuiné, S., Li-Beisson, Y. & Peltier, G. (2021) Alternative electron pathways of photosynthesis drive the algal CO_2 concentrating mechanism. *bioRxiv*. doi.org/10.1101/2021.02.25.432959

Burlacot, A., Richaud, P., Gosset, A., Li-Beisson, Y. & Peltier, G. (2020) Algal photosynthesis converts nitric oxide into nitrous oxide. *Proceedings of the National Academy of Sciences of the United States of America*, 117, 2704–2709.

Büsch, A., Friedrich, B. & Cramm, R. (2002) Characterization of the *norB* gene, encoding nitric oxide reductase, in the nondenitrifying cyanobacterium *Synechocystis* sp. strain PCC6803. *Applied and Environmental Microbiology*, 68, 668–672.

Calzadilla, P.I. & Kirilovsky, D. (2020) Revisiting cyanobacterial state transitions. *Photochemical & Photobiological Sciences*, 19, 585–603.

Cassier-Chauvat, C. & Chauvat, F. (2014) Function and regulation of ferredoxins in the cyanobacterium, *Synechocystis* PCC6803: recent advances. *Life*, 4, 666–680.

Chemla, Y., Peeri, M., Heltberg, M.L., Eichler, J., Jensen, M.H., Tuller, T. et al. (2020) A possible universal role for mRNA secondary structure in bacterial translation revealed using a synthetic operon. *Nature Communications*, 11, 4827.

Choi, J.S., Kim, D.S., Lee, J., Kim, S.J., Kim, S.I., Kim, Y.H. et al. (2000) Proteome analysis of light-induced proteins in *Synechocystis* sp. PCC 6803: identification of proteins separated by 2D-PAGE using N-terminal sequencing and MALDI-TOF MS. *Molecules and Cells*, 10, 705–711.

Choi, M., Chang, C. & Vitek, O. (2014) MSstats: protein significance analysis in DDA, SRM and DIA for label-free or label-based proteomics eeriments. R Packag version 260

Choi, M., Chang, C.-Y., Clough, T., Broudy, D., Killeen, T., MacLean, B. et al. (2014) MSstats: an R package for statistical analysis of quantitative mass spectrometry-based proteomic experiments. *Bioinformatics*, 30, 2524–2526.

Daley, S.M.E., Kappell, A.D., Carrick, M.J. & Burnap, R.L. (2012) Regulation of the cyanobacterial CO_2-concentrating mechanism involves internal sensing of $NADP^+$ and α-ketogutarate levels by transcription factor CcmR. *PLoS One*, 7, e41286.

Deutsch, E.W., Csordas, A., Sun, Z., Jarnuczak, A., Perez-Riverol, Y., Ternent, T. et al. (2017) The ProteomeXchange consortium in 2017: supporting the cultural change in proteomics public data deposition. *Nucleic Acids Research*, 45, D1100–D1106.

Ermakova, M., Huokko, T., Richaud, P., Bersanini, L., Howe, C.J., Lea-Smith, D.J. et al. (2016) Distinguishing the roles of thylakoid respiratory terminal oxidases in the cyanobacterium *Synechocystis* sp. PCC 6803. *Plant Physiology*, 171, 1307–1319.

Exss-Sonne, P., Tölle, J., Bader, K.P., Pistorius, E.K. & Michel, K.P. (2000) The IdiA protein of *Synechococcus* sp. PCC 7942 functions in protecting the acceptor side of photosystem II under oxidative stress. *Photosynthesis Research*, 63, 145–157.

Flores, E., Guerrero, M.G. & Losada, M. (1983) Photosynthetic nature of nitrate uptake and reduction in the cyanobacterium *Anacystis nidulans*. *Biochimica et Biophysica Acta - Bioenergetics*, 722, 408–416.

Flores, E. & Herrero, A. (2005) Nitrogen assimilation and nitrogen control in cyanobacteria. *Biochemical Society Transactions*, 33, 164–167.

Forchhammer, K. & Selim, K.A. (2019) Carbon/nitrogen homeostasis control in cyanobacteria. *FEMS Microbiology Reviews*, 44, 33–53.

Frischkorn, K.R., Haley, S.T. & Dyhrman, S.T. (2019) Transcriptional and proteomic choreography under phosphorus deficiency and re-supply in the N_2 fixing cyanobacterium *Trichodesmium erythraeum*. *Frontiers in Microbiology*, 10, 1–13.

Fry, E.S., Kattawar, G.W. & Pope, R.M. (1992) Integrating cavity absorption meter. *Applied Optics*, 31, 2055–2065.

Gaber, A., Tamoi, M., Takeda, T., Nakano, Y. & Shigeoka, S. (2001) NADPH-dependent glutathione peroxidase-like proteins (Gpx-1, Gpx-2) reduce unsaturated fatty acid hydroperoxides in *Synechocystis* PCC 6803. *FEBS Letters*, 499, 32–36.

Gaber, A., Yoshimura, K., Tamoi, M., Takeda, T., Nakano, Y. & Shigeoka, S. (2004) Induction and functional analysis of two reduced nicotinamide adenine dinucleotide phosphate-dependent glutathione peroxidase-like proteins in *Synechocystis* PCC 6803 during the progression of oxidative stress. *Plant Physiology*, 136, 2855–2861.

Halbeisen, R.E. & Gerber, A.P. (2009) Stress-dependent coordination of transcriptome and translatome in yeast. *PLoS Biology*, 7, e1000105.

Heinz, S., Liauw, P., Nickelsen, J. & Nowaczyk, M. (2016) Analysis of photosystem II biogenesis in cyanobacteria. *Biochimica et Biophysica Acta - Bioenergetics*, 1857, 274–287.

Helman, Y., Tchernov, D., Reinhold, L., Shibata, M., Ogawa, T., Schwarz, R. et al. (2003) Genes encoding A-type flavoproteins are essential for photoreduction of O_2 in cyanobacteria. *Current Biology*, 13, 230–235.

Hihara, Y., Kamei, A., Kanehisa, M., Kaplan, A. & Ikeuchi, M. (2001) DNA microarray analysis of cyanobacterial gene expression during acclimation to high light. *Plant Cell*, 13, 793–806.

Hille, F., Richter, H., Wong, S.P., Bratovič, M., Ressel, S. & Charpentier, E. (2018) The biology of CRISPR-Cas: backward and forward. *Cell*, 172, 1239–1259.

Ishii, A. & Hihara, Y. (2008) An AbrB-like transcriptional regulator, Sll0822, is essential for the activation of nitrogen-regulated genes in *Synechocystis* sp. PCC 6803. *Plant Physiology*, 148, 660–670.

Jahn, M., Vialas, V., Karlsen, J., Maddalo, G., Edfors, F., Forsström, B. et al. (2018) Growth of cyanobacteria is constrained by the abundance of light and carbon assimilation proteins. *Cell Reports*, 25, 4827.

Käll, L., Canterbury, J.D., Weston, J., Noble, W.S. & MacCoss, M.J. (2007) Semi-supervised learning for peptide identification from shotgun proteomics datasets. *Nature Methods*, 4, 923–925.

Kaneko, T., Sato, S., Kotani, H., Tanaka, A., Asamizu, E., Nakamura, Y. et al. (1996) Sequence analysis of the genome of the unicellular cyanobacterium *synechocystis* sp. strain PCC6803. II. Sequence determination of the entire genome and assignment of potential protein-coding regions (supplement). *DNA Research*, 3, 109–136.

Kirilovsky, D. & Kerfeld, C.A. (2016) Cyanobacterial photoprotection by the orange carotenoid protein. *Nature Plants*, 2, 16180.

Klähn, S., Orf, I., Schwarz, D., Matthiessen, J.K.F., Kopka, J., Hess, W.R. et al. (2015) Integrated transcriptomic and metabolomic characterization of the low-carbon response using an *ndhR* mutant of *Synechocystis* sp . PCC 6803. *Plant Physiology*, 169, 1540–1556.

Klotz, A., Reinhold, E., Doello, S. & Forchhammer, K. (2015) Nitrogen starvation acclimation in *Synechococcus elongatus*: redox-control and the role of nitrate reduction as an electron sink. *Life*, 5, 888–904.

Kufryk, G., Hernandez-Prieto, M.A., Kieselbach, T., Miranda, H., Vermaas, W. & Funk, C. (2008) Association of small CAB-like proteins (SCPs) of *Synechocystis* sp. PCC 6803 with photosystem II. *Photosynthesis Research*, 95, 135–145.

Latifi, A., Ruiz, M. & Zhang, C.C. (2009) Oxidative stress in cyanobacteria. *FEMS Microbiology Reviews*, 33, 258–278.

Laughlin, T.G., Savage, D.F. & Davies, K.M. (2020) Recent advances on the structure and function of NDH-1: the complex I of oxygenic photosynthesis. *Biochimica et Biophysica Acta - Bioenergetics*, 1861, 148254.

Leplat, C., Champeimont, R., Saenkham, P., Cassier-Chauvat, C., Jean-Christophe, A. & Chauvat, F. (2013) Genome-wide transcriptome analysis of hydrogen production in the cyanobacterium *Synechocystis*: towards the identification of new players. *International Journal of Hydrogen Energy*, 38, 1866–1872.

Li, L., Aro, E.M. & Millar, A.H. (2018) Mechanisms of photodamage and protein turnover in photoinhibition. *Trends in Plant Science*, 23, 667–676.

Li, H., Singh, A. K., McIntyre, L. M., & Sherman, L. A. (2004). Differential gene expression in response to hydrogen peroxide and the putative PerR regulon of Synechocystis sp. *strain PCC 6803*. *Journal of bacteriology*, 186, 3331–3345.

Macintyre, H.L., Kana, T.M. & Geider, R.J. (2000) The effect of water motion on short-term rates of photosynthesis by marine phytoplankton. *Trends in Plant Science*, 5, 12–17.

MacLean, B., Tomazela, D.M., Shulman, N., Chambers, M., Finney, G.L., Frewen, B. et al. (2010) Skyline: an open source document editor for creating and analyzing targeted proteomics experiments. *Bioinformatics*, 26, 966–968.

Maier, T., Güell, M. & Serrano, L. (2009) Correlation of mRNA and protein in complex biological samples. *FEBS Letters*, 583, 3966–3973.

Michel, K.P., Thole, H.H. & Pistorius, E.K. (1996) IdiA, a 34 kDa protein in the cyanobacteria *Synechococcus* sp. strains PCC 6301 and PCC 7942, is required for growth under iron and manganese limitations. *Microbiology*, 142, 2635–2645.

Muramatsu, M. & Hihara, Y. (2012) Acclimation to high-light conditions in cyanobacteria: from gene expression to physiological responses. *Journal of Plant Research*, 125, 11–39.

Muro-Pastor, A.M. & Hess, W.R. (2020) Regulatory RNA at the crossroads of carbon and nitrogen metabolism in photosynthetic cyanobacteria. *Biochimica et Biophysica Acta - Gene Regulatory Mechanisms*, 1863, 194477.

Mustila, H., Allahverdiyeva, Y., Isojärvi, J., Aro, E.M. & Eisenhut, M. (2014) The bacterial-type [4Fe-4S] ferredoxin 7 has a regulatory function under photooxidative stress conditions in the cyanobacterium *Synechocystis* sp. PCC 6803. *Biochimica et Biophysica Acta - Bioenergetics*, 1837, 1293–1304.

Mustila, H., Paananen, P., Battchikova, N., Santana-Sánchez, A., Muth-Pawlak, D., Hagemann, M. et al. (2016) The flavodiiron protein Flv3 functions as a homo-oligomer during stress acclimation and is distinct from the Flv1/Flv3 hetero-oligomer specific to the O_2 photoreduction pathway. *Plant and Cell Physiology*, 57, 1468–1483.

Nie, L., Wu, G., Culley, D.E., Scholten, J.C.M. & Zhang, W. (2007) Integrative analysis of transcriptomic and proteomic data: challenges, solutions and applications. *Critical Reviews in Biotechnology*, 27, 63–75.

Nikkanen, L., Santana Sánchez, A., Ermakova, M., Rögner, M., Cournac, L. & Allahverdiyeva, Y. (2020) Functional redundancy between flavodiiron proteins and NDH-1 in *Synechocystis* sp. PCC 6803. *The Plant Journal*, 103, 1460–1476.

Orf, I., Schwarz, D., Kaplan, A., Kopka, J., Hess, W.R., Hagemann, M. et al. (2016) CyAbrB2 contributes to the transcriptional regulation of low CO_2 acclimation in *synechocystis* sp. PCC 6803. *Plant and Cell Physiology*, 57, 2232–2243.

Palenik, B. (2015) Molecular mechanisms by which marine phytoplankton respond to their dynamic chemical environment. *Annual Review of Marine Science*, 7, 325–340.

Peltier, G., Aro, E.M. & Shikanai, T. (2016) NDH-1 and NDH-2 plastoquinone reductases in oxygenic photosynthesis. *Annual Review of Plant Biology*, 67, 55–80.

Pérez-Pérez, M.E., Martín-Figueroa, E. & Florencio, F.J. (2009) Photosynthetic regulation of the cyanobacterium *synechocystis* sp. PCC 6803 thioredoxin system and functional analysis of TrxB (Trx x) and TrxQ (Trx y) thioredoxins. *Molecular Plant*, 2, 270–283.

Perkins, D.N., Pappin, D.J., Creasy, D.M. & Cottrell, J.S. (1999) Probability-based protein identification by searching sequence databases using mass spectrometry data. *Electrophoresis*, 20, 3551–3567.

Riediger, M., Kadowaki, T., Nagayama, R., Georg, J., Hihara, Y. & Hess, W. R. (2019) Biocomputational analyses and experimental validation identify the regulon controlled by the redox-responsive transcription factor RpaB. *iScience*, 15, 316–331.

Rippka, R., Deruelles, J. & Waterbury, J.B. (1979) Generic assignments, strain histories and properties of pure cultures of cyanobacteria. *Journal of General Microbiology*, 111, 1–61.

Robles-Rengel, R., Florencio, F.J. & Muro-Pastor, M.I. (2019) Redox interference in nitrogen status via oxidative stress is mediated by 2-oxoglutarate in cyanobacteria. *The New Phytologist*, 224, 216–228.

Roncel, M., Kirilovsky, D., Guerrero, F., Serrano, A. & Ortega, J.M. (2012) Photosynthetic cytochrome *c*550. *Biochimica et Biophysica Acta - Bioenergetics*, 1817, 1152–1163.

Santana-Sanchez, A., Solymosi, D., Mustila, H., Bersanini, L., Aro, E.-M. & Allahverdiyeva, Y. (2019) Flavodiiron proteins 1-to-4 function in versatile combinations in O_2 photoreduction in cyanobacteria. *eLife*, 8, e45766.

Schmitt, F.J., Renger, G., Friedrich, T., Kreslavski, V.D., Zharmukhamedov, S.K., Los, D.A. et al. (2014) Reactive oxygen species: re-evaluation of generation, monitoring and role in stress-signaling in phototrophic organisms. *Biochimica et Biophysica Acta - Bioenergetics*, 1837, 835–848.

Scholz, I., Lange, S.J., Hein, S., Hess, W.R. & Backofen, R. (2013) CRISPR-Cas systems in the cyanobacterium *Synechocystis* sp. PCC6803 exhibit distinct processing pathways involving at least two Cas6 and a Cmr2 protein. *PLoS One*, 8, e56470.

Schubert, H., Sagert, S. & Forster, R.M. (2001) Evaluation of the different levels of variability in the underwater light field of a shallow estuary. *Helgoland Marine Research*, 55, 12–22.

Schuller, J.M., Saura, P., Thiemann, J., Schuller, S.K., Gamiz-Hernandez, A. P., Kurisu, G. et al. (2020) Redox-coupled proton pumping drives carbon concentration in the photosynthetic complex I. *Nature Communications*, 11, 494.

Shen, J.R., Qian, M., Inoue, Y. & Burnap, R.L. (1998) Functional characterization of *Synechocystis* sp. PCC 6803 Δ*psbU* and Δ*psbV* mutants reveals important roles of cytochrome *c*-550 in cyanobacterial oxygen evolution. *Biochemistry*, 37, 1551–1558.

Sontheimer, E.J. & Marraffini, L.A. (2010) CRISPR intereference: RNA-directed adaptive immunity in bacteria and archaea. *Nature Reviews. Genetics*, 11, 181–190.

Spät, P., Barske, T., Maček, B. & Hagemann, M. (2021) Alterations in the CO_2 availability induce alterations in the phosphoproteome of the cyanobacterium *Synechocystis* sp. PCC 6803. *New Phytology*. https://doi.org/10.1111/nph.17423

Tan, X., Hou, S., Song, K., Georg, J., Klähn, S., Lu, X. et al. (2018) The primary transcriptome of the fast-growing cyanobacterium *Synechococcus elongatus* UTEX 2973. *Biotechnology for Biofuels*, 11, 1–17.

Teikari, J., Österholm, J., Kopf, M., Battchikova, N., Wahlsten, M., Aro, E. M. et al. (2015) Transcriptomic and proteomic profiling of *Anabaena* sp. strain 90 under inorganic phosphorus stress. *Applied and Environmental Microbiology*, 81, 5212–5222.

Tichy, M. & Vermaas, W. (1999) In vivo role of catalase-peroxidase in *Synechocystis* sp. strain PCC 6803. *Journal of Bacteriology*, 181, 1875–1882.

Tölle, J., Michel, K.P., Kruip, J., Kahmann, U., Preisfeld, A. & Pistorius, E.K. (2002) Localization and function of the IdiA homologue Slr1295 in the cyanobacterium *Synechocystis* sp. strain PCC 6803. *Microbiology*, 148, 3293–3305.

Toyoshima, M., Tokumaru, Y., Matsuda, F. & Shimizu, H. (2020) Assessment of protein content and phosphorylation level in *Synechocystis* sp. PCC 6803 under various growth conditions using quantitative phosphoproteomic analysis. *Molecules*, 25, 3582.

Vizcaíno, J.A., Csordas, A., Del-Toro, N., Dianes, J.A., Griss, J., Lavidas, I. et al. (2016) 2016 update of the PRIDE database and its related tools. *Nucleic Acids Research*, 44, D447–D456.

Vogel, C. & Marcotte, E.M. (2012) Insights into the regulation of protein abundance from proteomic and transcriptomic analyses. *Nature Reviews. Genetics*, 13, 227–232.

Vuorijoki, L., Isojärvi, J., Kallio, P., Kouvonen, P., Aro, E.M., Corthals, G.L. et al. (2016) Development of a quantitative SRM-based proteomics method to study iron metabolism of *Synechocystis* sp. PCC 6803. *Journal of Proteome Research*, 15, 266–279.

Waldbauer, J.R., Rodrigue, S., Coleman, M.L. & Chisholm, S.W. (2012) Transcriptome and proteome dynamics of a light-dark synchronized bacterial cell cycle. *PLoS One*, 7, e43432.

Wegener, K.M., Singh, A.K., Jacobs, J.M., Elvitigala, T., Welsh, E.A., Keren, N. et al. (2010) Global proteomics reveal an atypical strategy for carbon/nitrogen assimilation by a cyanobacterium under diverse environmental perturbations. *Molecular and Cellular Proteomics*, 9, 2678–2689.

Wegener, K.M., Welsh, E.A., Thornton, L.E., Keren, N., Jacobs, J.M., Hixson, K. K. et al. (2008) High sensitivity proteomics assisted discovery of a novel operon involved in the assembly of photosystem II, a membrane protein complex. *The Journal of Biological Chemistry*, 283, 27829–27837.

Wilson, A., Ajlani, G., Verbavatz, J.M., Vass, I., Kerfeld, C.A. & Kirilovsky, D. (2006) A soluble carotenoid protein involved in phycobilisome-related energy dissipation in cyanobacteria. *Plant Cell*, 18, 992–1007.

Xiong, Q., Feng, J., Li, S.T., Zhang, G.Y., Qiao, Z.X., Chen, Z. et al. (2015) Integrated transcriptomic and proteomic analysis of the global response of *Synechococcus* to high light stress. *Molecular and Cellular Proteomics*, 14, 1038–1053.

Zak, E. & Pakrasi, H.B. (2000) The BtpA protein stabilizes the reaction center proteins of photosystem I in the cyanobacterium *Synechocystis* sp. PCC 6803 at low temperature. *Plant Physiology*, 123, 215–222.

Zavřel, T., Faizi, M., Loureiro, C., Poschmann, G., Stühler, K., Sinetova, M. et al. (2019) Quantitative insights into the cyanobacterial cell economy. *eLife*, 8, 1–29.

SUPPORTING INFORMATION

Additional supporting information may be found online in the Supporting Information section at the end of this article.

How to cite this article: Mustila, H., Muth-Pawlak, D., Aro, E.-M., Allahverdiyeva, Y. (2021) Global proteomic response of unicellular cyanobacterium *Synechocystis* sp. PCC 6803 to fluctuating light upon CO_2 step-down. *Physiologia Plantarum*, 173(1), 305–320. Available from: https://doi.org/10.1111/ppl.13482